DAILY EGG PRODUCTION, SPAWNING BIOMASS AND RECRUITMENT FOR THE CENTRAL SUBPOPULATION OF NORTHERN ANCHOVY 1981–2009

BENJAMIN E. FISSEL
NOAA, Alaska Fisheries Science Center
Economics and Social Sciences Research Program
7600 Sand Point Way NE
Seattle, WA 98115
Email: Ben.Fissel@noaa.gov

NANCY C. H. LO
Fisheries Resources Division
Southwest Fisheries Science Center
8604 La Jolla Shores Drive
La Jolla, CA 92037
Email: Nancy.Lo@noaa.gov

SAMUEL F. HERRICK JR.
Fisheries Resources Division
Southwest Fisheries Science Center
8604 La Jolla Shores Drive
La Jolla, CA 92037
Email: Sam.Herrick@noaa.gov

ABSTRACT

This paper updates estimates of critical stock assessment parameters for the central subpopulation of northern anchovy (*Engraulis mordax*). Ichthyoplankton data from the CalCOFI database were used to implement the historical egg production method and estimate annual mortality curves, from which daily egg production, and egg and larval mortality parameters were derived. Spawning biomass was estimated using historical data under the assumption of a constant daily specific fecundity. A Ricker recruitment model, augmented with environmental factors, was estimated based on historical data and used to predict recruitment using the new spawning biomass data. We found that egg densities were highly variable while larval densities have been persistently low since 1989. Recruitment estimation suggests that poor environmental conditions have potentially contributed to the low productivity. Mortality estimation reveals through an increasing egg mortality rate that low larval densities were primarily the result of high mortality during the pre-yolk-sac period.

1 INTRODUCTION

This paper updates the egg production statistics, spawning stock biomass, and recruitment time series from 1981–2009 for the central subpopulation of northern anchovy (*Engraulis mordax*) which occupies the California Current Ecosystem from San Francisco, California south to Punta Baja, Baja California, Mexico. It is the largest of the North Pacific subpopulations, and supported a significant U.S. fishery throughout the 1970s and 1980s. In 1978 the fishery came under federal management through the Pacific Fisheries Management Council's (PFMC) Northern Anchovy Fishery Management Plan (FMP) (PFMC 1978). In 1983 the FMP was amended (Amendment 5) in recognition that harvest should be adjusted annually to reflect the current status of the stock (PFMC 1983) and annual stock assessments were conducted to inform the annual U.S. anchovy harvest quota.

During the 1980s anchovy abundance started to decline as environmental conditions in the California Current ecosystem became less favorable for anchovy productivity. Concurrently, the conditions were favorable for the recovery of the Pacific sardine (*Sardinops sagax caerulea*) population and fishing effort began to shift from anchovy to sardine. With the shift in fishing effort from anchovy to sardine, conservation and management resources were redirected toward managing the expanding sardine fishery, and since 1995 no stock assessments have been conducted for the central subpopulation of northern anchovy (Jacobson et al. 1995). Our updated stock statistics are intended to provide valuable information about the anchovy's abundance trajectory over the past 15 years.

The core range of the bulk of the central subpopulation lies within the California Bight. Portions of the central subpopulation, thought to be smaller, exist north off the coast of San Francisco and Monterey, as well as south in Mexico (PFMC 2010). The bight has been regularly sampled by research cruises since 1949 and cataloged in the California Cooperative Oceanogrpahic and Fisheries Investigation (CalCOFI) database. The cruises conducted ichthyoplankton surveys at regular intervals, known as CalCOFI stations (Eber and Hewitt 1979). Anchovy ichthyoplankton from the surveys is preserved and later larvae are counted and lengths recorded, while eggs are only counted. The perserved lengths allow for the binning of larvae counts and aging, known as staging (Lo 1985a).

Numerous methods have been developed to analyze anchovy ichthyoplankton data (Hewitt 1981; Zweifel and Smith 1981; Hewitt and Methot 1982; Lasker 1985). The historical egg production method (HEPM) of Lo (1985a) is the method most amenable to the available CalCOFI data and is the closest to the daily egg production method (DEPM) (Lasker 1985) currently used for sardine (Lo et al. 2008). The HEPM is a method for estimating daily egg production (P_0) and other early life history mortality parameters of archived ichthyoplankton data. The HEPM was designed to provide indices of abundance for anchovy dating back to 1951 when no staging data for anchovy eggs were available. The DEPM was designed to estimate the spawning biomass for fish populations with indeterminate fecundity like anchovy and sardine (Hunter and Macewicz 1985) but requires

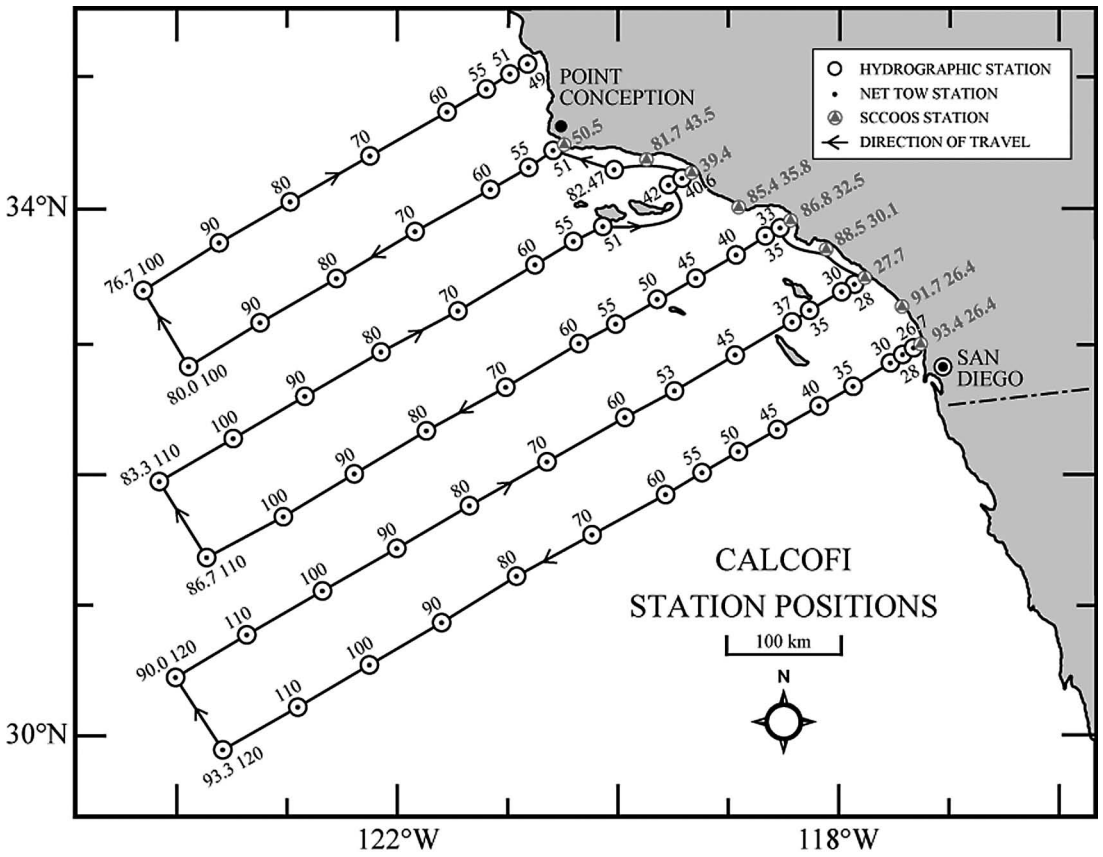

Figure 1. CalCOFI Stations in the core range. From: http://www.calcofi.org/cruises/stapos-depth/75stapattern.html accessed 08/23/10

staged eggs. While the more data intensive DEPM is preferred, HEPM provides an unbiased index of the daily egg production (Lo 1985a). The spawning stock biomass can then be estimated using daily egg production and daily specific fecundity of the stock (Parker 1980; Hewitt 1985).

The Ricker stock-recruitment model (Ricker 1954) can in turn be used to estimate recruitment from spawning biomass. The stock-recruitment relationships are typically highly variable as it spans the development phases of growth which are subject to a variety of influence. Theories explaining the dynamics of fishes often cite sensitivity in recruitment linked to environmental factors (Aydin 2005) as being a major driver. Previous research shows that anchovy recruitment success is influenced by wind stress driven upwelling (Husby and Nelson 1982; Peterman and Bradford 1987; Rykaczewski and Checkley 2008) and temperatures in the upper strata of the ocean (Butler 1989; Zweifel et al. 1976; Fiedler et al. 1986). We augment the Ricker model with wind stress and temperature to produce an environmental Ricker stock-recruitment model.

In this paper, daily egg production and mortality parameters were estimated using the HEPM. Spawning biomass was estimated using a model that regressed daily egg production on historical spawning biomass data (Jacobson et al. 1995) thereby assuming constant daily specific fecundity over time. Historical stock and environmental data was used to estimate the environmental Ricker stock-recruitment model and statistical validity of the model was explored. Bootstrapping was used to characterize variation in mortality.

2 DATA AND METHODS

2.1 Data

Data for the analysis was obtained from the CalCOFI database. Data were constrained to the central subpopulation's core range of the 75 CalCOFI stations (fig. 1) south of CalCOFI line 76.7 and north of line 93.3. Ichthyoplankton surveys over the core range from 1981–2009 were used. Our analysis was constrained to data collected during the peak anchovy spawning season between January and April (Hewitt and Methot 1982; Hewitt and Brewer 1983). We verified in our data that the peak spawning season has remained in this interval. The 75 stations analyzed had a median sampling frequency of 2.03 samples per year between Jan–April. Each cruise was weighted equally in our analysis.

Three different types of nets were used for ichthy-

oplankton surveys over 1981–2009. The CalBOBL or Bongo net (*CB*), the CalVET (*CVT*) and two connected CalVET nets called the PairOVET (*PV*) (*CVT* and *PV* are referred to collectively as *CVT/PV*)[1]. Our analysis utilizes ichthyoplankton samples from *CB* and *CVT* nets for 1981–1984 and *CB* and *PV* nets for 1985–2009.

2.2 Daily egg production

Egg production methods estimate the production of eggs at age zero, the time of spawning. Estimation of age-zero egg production per 10 m^2 (P_0) from the counts of eggs and larvae was carried out in a series of steps. Procedures for correcting raw ichthyoplankton counts and aging have followed the literature closely and incorporate previously derived parameters. Appendix A provides details on the methods used for egg and larval density construction and aging, and they are summarized in the following paragraph.

First, larvae were sorted into size classes based on preserved larval size. The size classes were 2.5 mm, 3.25 mm, 4.25 mm,…, 9.25 mm[2]. Extrusion and avoidance corrections were applied and standard haul factors were used to rescale egg and larval counts to a 10 m^2 area-density (appendix A1). The time it takes eggs to reach the developed stage, incubation time (t^I), was calculated using a temperature-dependent relationship (Lo 1983). A live larval length correction was made to preserved samples, and live lengths were used in a temperature and month-dependent two-stage Gompertz growth curve (GGC) (Lo 1983; Hewitt and Methot 1980) to estimate larval age (t) (appendix A2). The first stage of the GGC spans the first three larval classes (2.5 mm, 3.25 mm, 4.25 mm) and is designed to model growth over the period of yolk-sac consumption. The second stage of the GGC covers post-yolk-sac consumption growth (5.25 mm,…, 9.25 mm) when larvae must seek out food in their environment. Aggregation of the samples over cruises and stations yielded annual age and density statistics for the region. The daily larval production (*DLP*) is the daily production of larvae in a size class per 10 m^2 area-density, and was constructed as the standing stock of larvae in a size class over the number of days that larvae spend in that size class as determined by the growth curve.

Methods for the estimation of the mortality curves are presented in the following subsection 2.2.1. However, it is useful to first summarize the approach. Figure 2 displays a conceptual graph of the HEPM estimation process. First, daily larval production and corresponding size

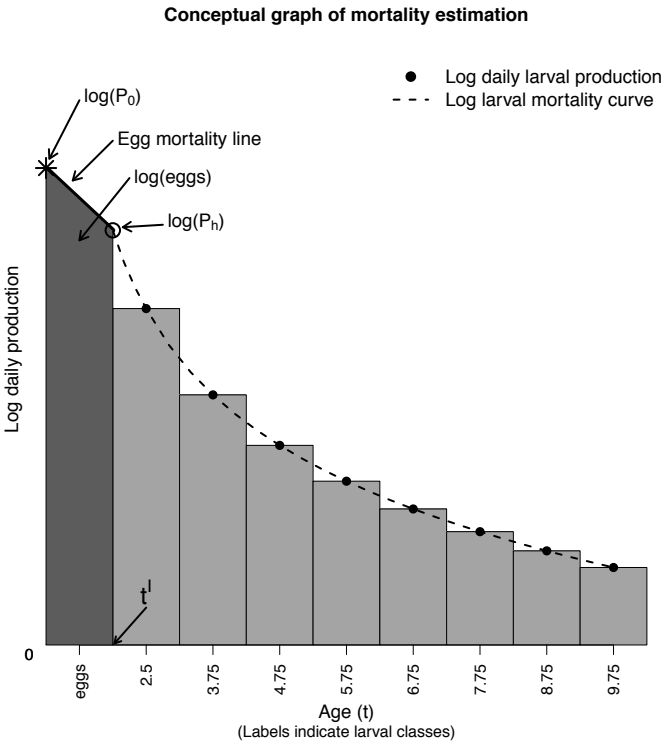

Figure 2. Conceptual graph of HEP mortality estimation, on log-linear axes.

class ages were used to construct larval mortality curves (Lo 1985c). The mortality curve was parameterized such that the fitted *DLP* at the age of incubation time, $t = t^I$, gives the production at the time of hatching (P_h). Under the assumption that the egg instantaneous mortality rate (IMR) is constant across egg stages[3], the egg IMR can be found as the value that is consistent with the observed standing stock of (unstaged) eggs (the dark shaded region in fig. 2). Having obtained the egg IMR over the time of incubation, production of eggs at age 0 (P_0), can be estimated using the egg mortality curve from P_h back to the time of spawning.

Residual bootstrapping (MacKinnon 2006) of the annual mortality curves was used to provide annual estimates of variability for larval and egg mortality parameters (appendix B). Bootstrap based variation is reported as 95% confidence intervals (CIs) which were constructed by taking the 0.025 and 0.975 quantiles of the relevant bootstrapped distribution. Details on the bootstrap procedure are provided in appendix B.

2.2.1 Mortality curves and daily egg production. An annual Pareto type mortality curve was used to model the mortality of larvae from the time of hatching. The variables of daily larval production, $dlp_{c,s}$, average age of larvae ($t_{c,s}$) and incubation time t^I_s for larval class c in year s (see appendix A) are used to identify the parameters

[1]Further details on sampling procedures and nets are available from the Southwest Fisheries Science Center (SWFSC), CalCOFI, Smith and Richardson (1977).

[2]Larval class sizes greater than 9.25 mm were discarded because mature larvae are more adept at avoiding nets thereby introducing significant bias into production calculations (appendix A3).

[3]This assumption was verified in Lo (1985a) for select years.

in the model. Each year was estimated independently using the equation:

$$dlp_{c,s} = P_{h,s}\left(t_{c,s}/t^{I}_{s}\right)^{-\beta_s} + \varepsilon_{c,s} \quad (1)$$

where the mortality curve parameterization was chosen by Lo (1985a) so that $P_{h,s}$ is the production at the time of hatching ($t = t^{I}_{s}$), and β_s is the coefficient of the larval instantaneous mortality rate. The larval instantaneous mortality rate decreases as larvae age, and at age t is β/t (Hewitt and Brewer 1983). We assume the error term, $\varepsilon_{c,s}$, is distributed with a mean-zero, however, we allow for heteroskedasticity across ages through our bootstrap methods (appendix B). Equation 1 was fit using nonlinear least squares (NLS). A grid search over initial conditions was performed and the parameters that minimized the sum-of-squared errors were used. A residual bootstrap of equation 1 was used to construct 95% CIs for β_s and $P_{h,s}$ (appendix B).

An exponential curve, which applied a constant instantaneous mortality rate (IMR), α, was used to model egg mortality to $P_{h,s}$: $\log(P_0) - \alpha^* t = \log(\text{egg production at age } t)$, for $t \in (0, t^I)$, where $\log(P_0) - \alpha^* t^I = \log(P_h)$[4]. Manipulation of the definition for the observed standing stock of eggs and the production at the time of hatching (Lo 1985a) yields a definition that was used to calculate the egg IMR:

$$\frac{m_s}{P_{h,s}} = \frac{e^{\alpha_s * t^I_s} - 1}{\alpha_s} \quad (2)$$

where m_s is the observed corrected standing stock of eggs, and the egg IMR, α_s, was estimated by iterative method. Daily egg production can now be estimated as the production at time zero, $P_{0,s}$, necessary to produce the estimated $P_{h,s}$ give the egg mortality rate α_s, and the time it takes to incubate t^I:

$$P_{0,s} = P_{h,s}\, e^{\alpha_s * t^I_s} \quad (3)$$

Ninety-five percent CIs for α_t and $P_{0,s}$ were derived by re-estimating equations 2 and 3 at each iteration of the larval bootstrap (appendix B).

2.3 Spawning stock biomass estimation

To obtain estimates of *SSB* overlapping, historical data from Jacobson et al. (1995) was used and daily specific fecundity, D_s, was assumed constant over time so that the SSB_s is proportional to $P_{0,s}$. With this assumption a simple linear regression without a constant is estimated:

$$SSB_s = \gamma\, P_{0,s} 10^5 \Lambda + \eta D1_s + \epsilon_s \quad (4)$$

where $P_{0,s}10^5$ is the daily egg production per km^2 Λ is the area of the core CalCOFI region (approx. 200,500 km^2). From 1981–1986 data from south of the Mexican border was used by *National Marine Fisheries Service's Southwest Fisheries Science Center* (SWFSC) to calculate SSB_s and other stock statistics, D1 is a categorical variable accounting for this: 1981–1986 ($D1$=1) and 1987-2009 ($D1$=0). The model was fit using the estimated $\widehat{P_{0,s}}$ (equation 3) and SSB_s from Jacobson et al. (1995) over the years 1981–1995. The fitted model was used to estimate the SSB_s from 1981–2009. The standard estimate of prediction error associated with ordinary least squares is reported.

2.4 Recruitment

Estimates of spawning stock biomass were used in conjunction with a Ricker curve to provide recruitment estimates and explore the impact of environmental conditions. The last anchovy stock assessment (Jacobson et al. 1995) provided estimates of both spawning stock biomass and recruitment for the years 1964–1995. Consistent with Jacobson et al. (1995) we refer to recruits as age-0 anchovy on July 1.

Two environmental factors were incorporated into our recruitment model, north-south (N-S) wind stress and sea surface temperature[5]. The Ricker stock-recruitment model was augmented with these variables in the exponential, which yields an environmental Ricker model:

$$R_s = A^* SSB_s * e^{B*SSB_s + \rho_1 * NSWind5_s + \rho_2 * tanom_s} + \varepsilon_s \quad (5)$$

where R_s is recruitment in year s, $tanom_s$ is the mean annual sea surface temperature (SST) anomay at Scripps pier and $NSWind5_s$ is the 5% quantile of the annual north-south wind stress anomaly distribution. Wind stress and sea surface temperature anomalies were computed as deviations from the monthly means across all available years. Recruitment and spawning biomass were normalized by their standard deviation, then fit using NLS over the stock and environmental data from 1964–1995. The standard Ricker curve ($\rho_1 = \rho_2 = 0$) was used as the null model, M^0, to evaluate the benefit of added

[4]Lo (1985a) provided two separate mortality estimates: first under the assumption of constant IMR to yolk-sac larval stage, and second constant through the first yolk-sac larval stage. Constant mortality through the first larval stage was a helpful assumption for the historical data used because *CVT/PV* samples were not present. The use of the *CVT/PV* nets in our data gives us sufficiently accurate sampling from from smaller larvae classes.

[5]North-south (N-S) wind stress data were obtained from the Environmental Research Division of the SWFSC through their Live Access Server http://www.pfeg.noaa.gov/products/las.html. The wind stress vectors are National Center for Environmental Predictions derived monthly wind stresses from the location 32.5 degrees north and 117.5 degrees west, and span 1948–2009. Data on Scripps pier SST data were obtained from the ocean informatics datazoo http://oceaninformatics.ucsd.edu/datazoo/data/ hosted by Scripps Institution of Oceanography.

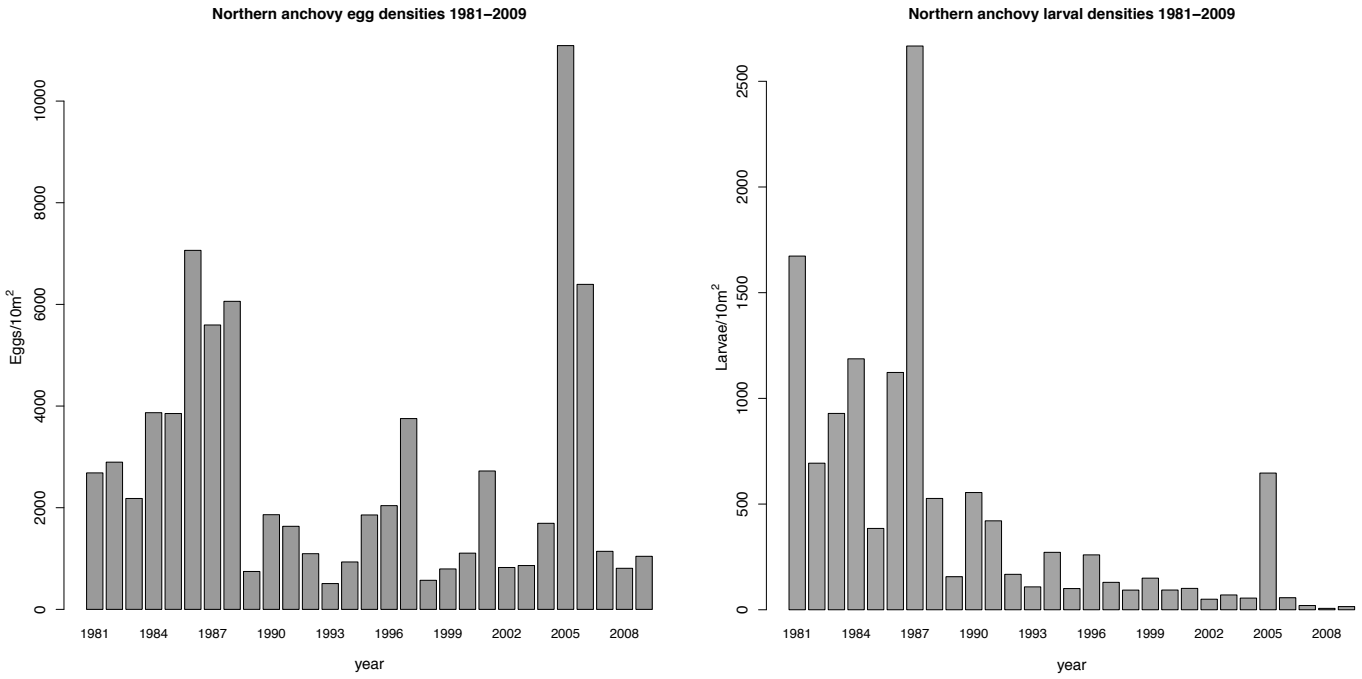

Figure 3. Annual egg and larval densities per 10 m² in the core CalCOFI region 1981–2009.

information from the full environmental Ricker model, M^{WT} (ρ_1, ρ_2 unconstrained). The Akaike information criterion (AIC) was used to compare the models. The ratio of likelihoods was formed as $L(M^0)/L(M^{WT}) = \exp((AIC^{WT} - AIC^0)/2)$, which is the likelihood that the constrained null model minimizes the information loss relative to the unconstrained model that uses the environmental factors (Burnham, K. P. and D. R. Anderson (2002)), which we denote by $I(M^{WT}) \leq I(M^0)$. Similar AIC probability calculations were carried out on different model specification to assess the relative contribution of the individual environmental factors. *SSB* estimates obtained from equation 4 were used with the fitted environmental Ricker model to estimate recruitment from 1981–2009.

3 RESULTS

Annual density plots for the core CalCOFI stations show the temporal variation of eggs and larvae (fig. 3, table 1). Since approximately 1989, egg densities in general, have been lower although more highly variable than the years preceding. Prior to 1989 densities ranged from 2182/10 m² to 7063/10 m² with a mean of 4276/10 m², while later densities showed a range of 508/10 m² to 11091/10 m² and a mean of 2070/10 m² with pronounced episodes of high density particularly in 2005–2006 (table 1). In contrast, larvae densities have declined fairly steadily since 1989 except for 2005 when an increase in larval density was associated with the correspondingly high egg density (fig. 3 right panel). Larval densities ranged from 394.1/10 m² to 2870.2/10 m² with a mean of 1177.9/10 m² prior to 1989, and after had a range of 6.3/10 m² to 648.8/10 m² and a mean of 166.3/10 m² with pronounced episodes of high density particularly in 2005–2006 (table 1). Larvae densities do not track the dynamics of egg densities closely and are considerably smaller than densities observed through the mid to late 1980s; similar to patterns in 1951–1982 (Lo 1985a).

Egg density closely mirrors P_0 (figs. 3 and 4, table 1). P_0 displays high post-1989 production around 1997, 2001 and a pronounced episode of high density in 2005. In the early '80s *DEP* appears comparatively low in contrast to the relative egg density owing to the low egg IMR (α) during that period (fig. 4 upper-right panel, table 1). The larval mortality coefficient (β) has been variable but has maintained an average value of approximately −1.89 (fig. 4 lower right panel). In contrast, the egg IMR has been increasing from low levels in the early '80s to over 2 in the late 2000s. A linear time trend has been superimposed on the egg IMR time series and shows that the egg IMR has been increasing by approximately 0.06 per year. Bootstrap CIs indicate that estimation of the egg IMR is more precise than the coefficient of larval mortality (fig. 4 right panel). The imprecision in the estimation of β is largely due to higher residual variance in the pre-yolk-sac-consumption larval phases (fig. B1). CIs for *DEP* indicate that the random variation in larval mortality does not significantly contribute to the observed pattern of *DEP*.

The spawning stock has shown periods of low biomass since 1989, but has been highly variable (fig. 5, table 2) with high post-1990 biomass around 1997, 2001

TABLE 1
Annual egg, larval and mortality statistics

Year	Egg dens. 10 m²	Larvae dens. 10 m²	β	P_h	α	P_0
1981	2685.26	1673.18	–1.96	1015.49	–0.04	912.35
			[–2.05,–1.84]	[866.5,987.3]	[–0.05,0.04]	[862,983]
1982	2896.23	693.44	–1.56	255.62	0.7	2279.5
			[–1.74,–1.23]	[186.4,280.1]	[0.61,0.8]	[2052,2495]
1983	2181.7	928.23	–2.02	616.87	0.24	1139.14
			[–2.17,–1.85]	[504.4,616.2]	[0.2,0.34]	[1061,1242]
1984	3869.8	1189.92	–1.82	598.47	0.56	2770.29
			[–1.92,–1.68]	[497,572.3]	[0.52,0.6]	[2601,2826]
1985	3853.01	394.07	–2.67	263.97	0.76	3177.28
			[–2.93,–2.06]	[191,282.3]	[0.71,0.88]	[3022,3578]
1986	7063.25	1144.54	–2.54	1196.2	0.43	4239.8
			[–2.69,–2.41]	[1129.7,1322.1]	[0.38,0.47]	[3993,4434]
1987	5595.11	2870.22	–2.2	1719.78	0.05	2021.12
			[–2.24,–2.15]	[1647.7,1714.2]	[0.05,0.08]	[1994,2069]
1988	6060.64	529.37	–2.22	282.93	0.82	5254.26
			[–2.48,–1.85]	[234.7,346]	[0.77,0.93]	[5011,5846]
1989	745.66	155.23	–2.06	80.66	0.62	542.7
			[–2.46,–1.2]	[43,87]	[0.5,0.82]	[464,656]
1990	1862.97	534.85	–1.96	313.13	0.5	1239.04
			[–2.18,–1.69]	[191.5,255.6]	[0.47,0.61]	[1133,1336]
1991	1634.47	421.06	–1.28	114.16	0.94	1658.65
			[–1.47,–0.91]	[80.1,129.2]	[0.82,1.05]	[1467,1791]
1992	1095.67	167.43	–1.89	85.94	0.98	1165.09
			[–2.35,–1.28]	[54.9,105.3]	[0.83,1.16]	[1011,1331]
1993	507.68	108.98	–1.52	37.55	0.87	476.87
			[–2.01,–0.68]	[18.7,56.5]	[0.68,1.23]	[403,642]
1994	932.9	271.69	–2.15	125.74	0.52	609.87
			[–2.5,–1.83]	[123.2,165.1]	[0.44,0.6]	[571,684]
1995	1857.66	99.84	–2.1	33.36	1.2	2270.21
			[–2.63,–1.26]	[28.8,59.5]	[1.24,1.56]	[2370,2927]
1996	2041.04	259.41	–2.65	156.04	0.86	1912.72
			[–2.93,–2.1]	[142.5,201.6]	[0.8,0.98]	[1836,2151]
1997	3753.55	130.25	–1.41	39.92	1.82	6884.84
			[–1.88,–0.83]	[22.8,56.1]	[1.57,1.94]	[5952,7319]
1998	572.02	85.71	–1.73	36.36	1.23	740.98
			[–2.08,–1.07]	[22.3,39.3]	[1.09,1.39]	[662,816]
1999	795.65	140.46	–1.97	71.66	0.64	581.51
			[–2.33,–1.5]	[45.3,77.2]	[0.53,0.75]	[499,646]
2000	1106.24	93.36	–2.47	55.3	1.06	1226.33
			[–2.85,–1.6]	[28.9,56.2]	[0.97,1.26]	[1127,1420]
2001	2722.55	101.16	–2.49	63.22	1.33	3689.34
			[–2.86,–1.65]	[31,57.7]	[1.22,1.46]	[3391,4010]
2002	823.98	49.78	–0.9	7.39	1.45	1200.32
			[–1.57,–0.28]	[4,14.3]	[1.24,1.7]	[1038,1401]
2003	862.19	70.08	–1.58	21.63	1.31	1150.54
			[–1.93,–1.05]	[14.3,27.5]	[1.22,1.5]	[1078,1307]
2004	1693.4	55.18	–2.61	33.95	1.51	2592.44
			[–2.99,–1.7]	[15.9,40]	[1.32,1.7]	[2274,2892]
2005	11091.12	648.81	–1.27	143.84	1.53	17161.25
			[–1.39,–1.12]	[137.3,171.6]	[1.57,1.67]	[17617,18637]
2006	6394.01	57.13	–1	9.41	2.34	14972.47
			[–1.8,0]	[3.5,26.3]	[1.99,2.73]	[12610,17272]
2007	1142.23	19.76	–1.13	3.41	2.03	2320.7
			[–1.87,–0.36]	[1.7,5.8]	[1.77,2.21]	[2023,2524]
2008	808.21	6.3	–1.92	1.89	2.02	1633.54
			[–2.46,–0.13]	[0.6,2.5]	[1.79,2.27]	[1447,1836]
2009	1044.16	14.8	–1.6	3.42	1.92	2012.21
			[–1.9,–0.32]	[2,4.5]	[1.86,2.15]	[1945,2249]

Egg and larval densities, the coefficient of the larval instantaneous mortality rate (IMR) (β), larval production at the time of hatching (P_h), egg IMR (α), and egg production at age at age zero per 10 m² (P_0). 95% bootstrap larval mortality confidence intervals are in brackets below the estimates.

and a pronounced episode of high biomass in 2005–2006. *SSB* has been comparatively lower in recent years. For the overlapping years of Jacobson et al. (1995) *SSB*, and our *SSB* estimates (fig. 5 left panel) there is some discrepancy but the respective trends are nearly identical ($R^2 = 0.825$) (table 3). The high biomass in 2005 is not without precedent; similar levels were seen around 1976. The parameter on *SSB*, γ, was significant at the

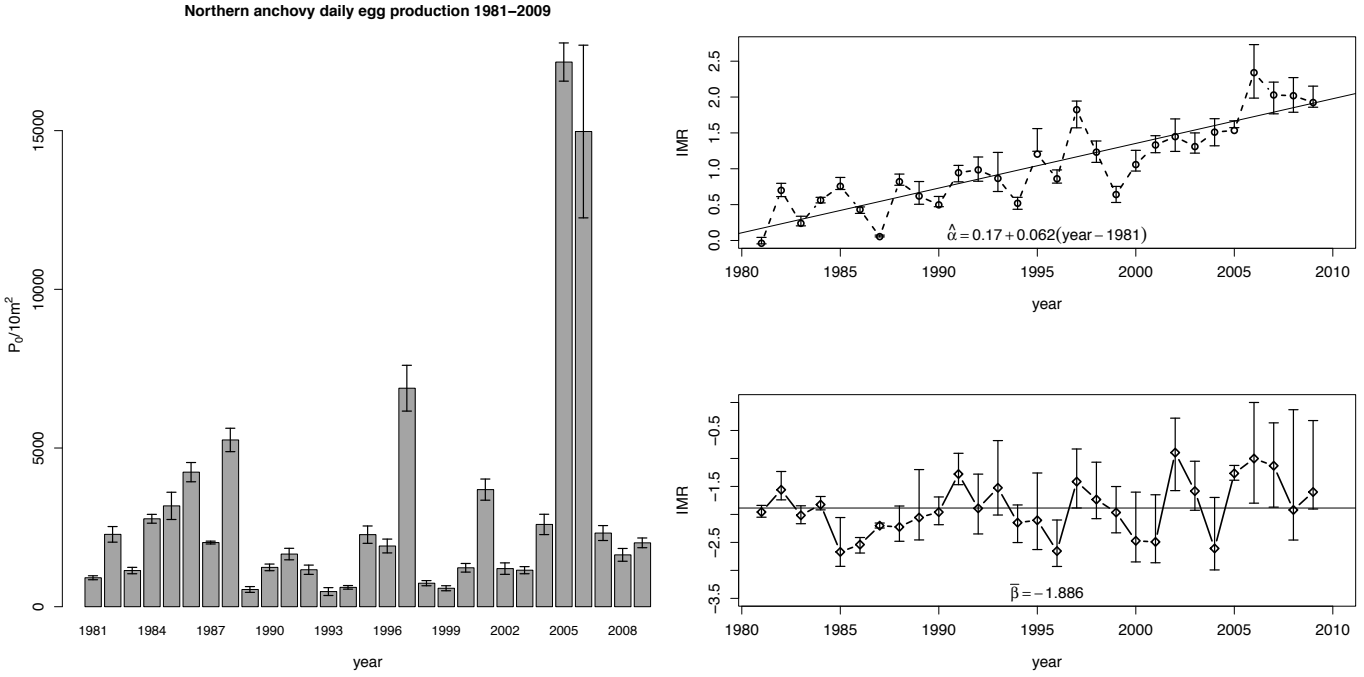

Figure 4. Annual daily egg production (P_0) (left panel) and egg IMR and coefficient of larval IMR (right panel). IMR regression coefficients displayed have a p-value ≤ 0.01. Error bars represent 95% bootstrapped larval mortality confidence intervals.

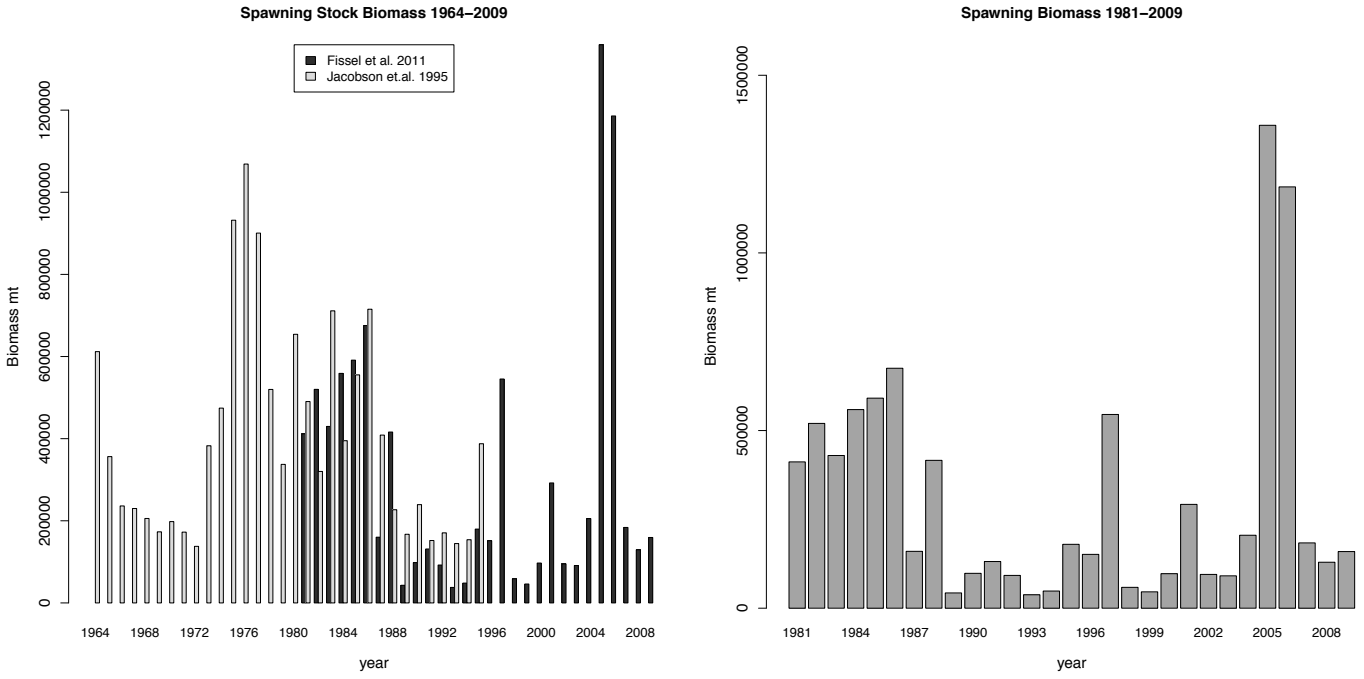

Figure 5. Comparison of historical and new annual spawning stock biomass (SSB_s) 1964–2009 (left panel). Annual spawning stock biomass 1981–2009 (right panel).

0.1% level (table 3) and can be roughly interpreted as the inverse of the daily specific fecundity per metric ton of *SSB*[6]. However, because of the assumptions and the reduced form nature of the regression γ may be capturing some latent changes over time. The implied daily specific fecundity (number of eggs produced per day per unit fish weight) per metric ton of biomass was $1/\gamma$ = 2.532 E+08. Aggregate specific fecundity can be obtained by multiplying this by the *SSB*.

[6]The fecundity parameters of the stock relate *SSB* to P_0 (Parker 1980; Hewitt 1985). The stocks sex-ratio (Q), the proportion of mature females spawning (F), and the average batch fecundity (E) relative to the mature female weight (W) give the daily specific fecundity, $1/\gamma = Q^*F^*(E/W)$. The daily specific fecundity and daily egg production can be related to the spawning biomass by: $P_0 = SSB^*(1/\gamma)$.

TABLE 2
Annual spawning biomass and recruitment statistics

Year	Spawning biomass	SSB Predic. Error	Recruitment	Wind S. .05 quant	Temp. mean
1981	411825.77	76469.05	670506.17	–0.848	0.512
1982	520106.22	68050.61	2292236.85	–1.728	0.022
1983	429787.65	74202.51	557112.61	–0.850	0.855
1984	558977.70	68459.06	1058457.90	–1.633	1.199
1985	591212.10	70215.62	482741.42	–0.320	0.109
1986	675365.57	80059.39	282065.59	–0.115	0.612
1987	160075.84	46971.72	393716.32	–0.732	0.451
1988	416146.22	122111.51	851826.18	–0.739	–0.113
1989	42983.16	12612.73	193872.87	–0.886	0.081
1990	98134.15	28795.91	240347.47	–0.790	0.786
1991	131368.04	38547.87	331156.59	–0.384	–0.144
1992	92276.93	27077.20	102489.76	–0.221	1.137
1993	37769.26	11082.79	38983.16	–0.056	1.149
1994	48302.66	14173.65	56698.02	–0.070	0.910
1995	179804.42	52760.76	594143.98	–1.170	0.681
1996	151490.66	44452.53	261865.36	–0.600	0.858
1997	545291.08	160007.02	352430.96	–1.067	2.084
1998	58686.52	17220.63	71883.07	–0.218	1.077
1999	46056.91	13514.67	311754.70	–0.906	–0.609
2000	97127.44	28500.51	154578.31	–0.273	0.582
2001	292202.02	85742.05	389139.87	–0.308	0.276
2002	95067.77	27896.13	224820.84	–0.487	0.290
2003	91125.05	26739.20	180510.05	–0.443	0.536
2004	205325.91	60249.63	195895.29	–0.344	1.237
2005	1359200.63	398835.88	117862.60	–0.214	1.166
2006	1185845.47	347967.55	190403.04	–0.378	0.996
2007	183803.71	53934.28	212452.88	–0.132	0.576
2008	129379.08	37964.24	175467.13	–0.100	0.427
2009	159370.30	46764.69	590413.16	–0.965	0.167

Spawning biomass (SSB) (mt) with prediction error and recruitment (mt). Mean sea surface temperature anomaly (Temp.) and the 0.05 quantile of the north-south wind stress anomaly distribution (Wind S.).

TABLE 3
Spawning Stock Biomass Regression

Coefficients	Estimate	Std. Error	t value	Pr(>|t|)
γ	3.950E-09	1.159E-09	3.408	0.00467**
η	3.396E+05	8.822E+04	3.849	0.00201**

Signif. codes: 0 '***' 0.001 '**' 0.01 '*' 0.05 '.' 0.1 ' ' >0.1
Residual standard error: 166500 on 13 deg. of freedom
Multiple R^2: 0.848, Adjusted R^2: 0.825
F-statistic: 36.34 on 2 and 13 DF, p-value: 4.749E-06

Coefficients of the regression are the inverse of the daily specific fecundity per metric ton of *SSB* (γ) and a categorical variable for the inclusion of Mexican data, 1981–1986 (η).

TABLE 4
Standard and environmental Ricker regressions

Standard Ricker M^0			Environmental Ricker M^{WT}		
Coefficient	Estimate	Std. Error	Coefficient	Estimate	Std.Error
A	1.3991*	0.5437	A	0.5659	0.2959
B	–0.5074*	0.1384	B	–0.5074**	0.1384
			ρ_1	–106.171**	36.359
			ρ_2	–0.5663*	0.2145
Resid std. error: 0.9815			Resid std error: 0.8026		
df = 3; AIC = 93.5538			df = 5; AIC = 82.4666		

Signif. codes: 0 '***' 0.001 '**' 0.01 '*' 0.05 '.' 0.1 ' ' >0.1

Comparison of the standard and environmental Ricker recruitment models with coefficient estimates for Ricker model parameters, the 0.05 quantile of the N-S wind stress anomaly (ρ_1) and mean sea surface temperature anomaly (ρ_2).

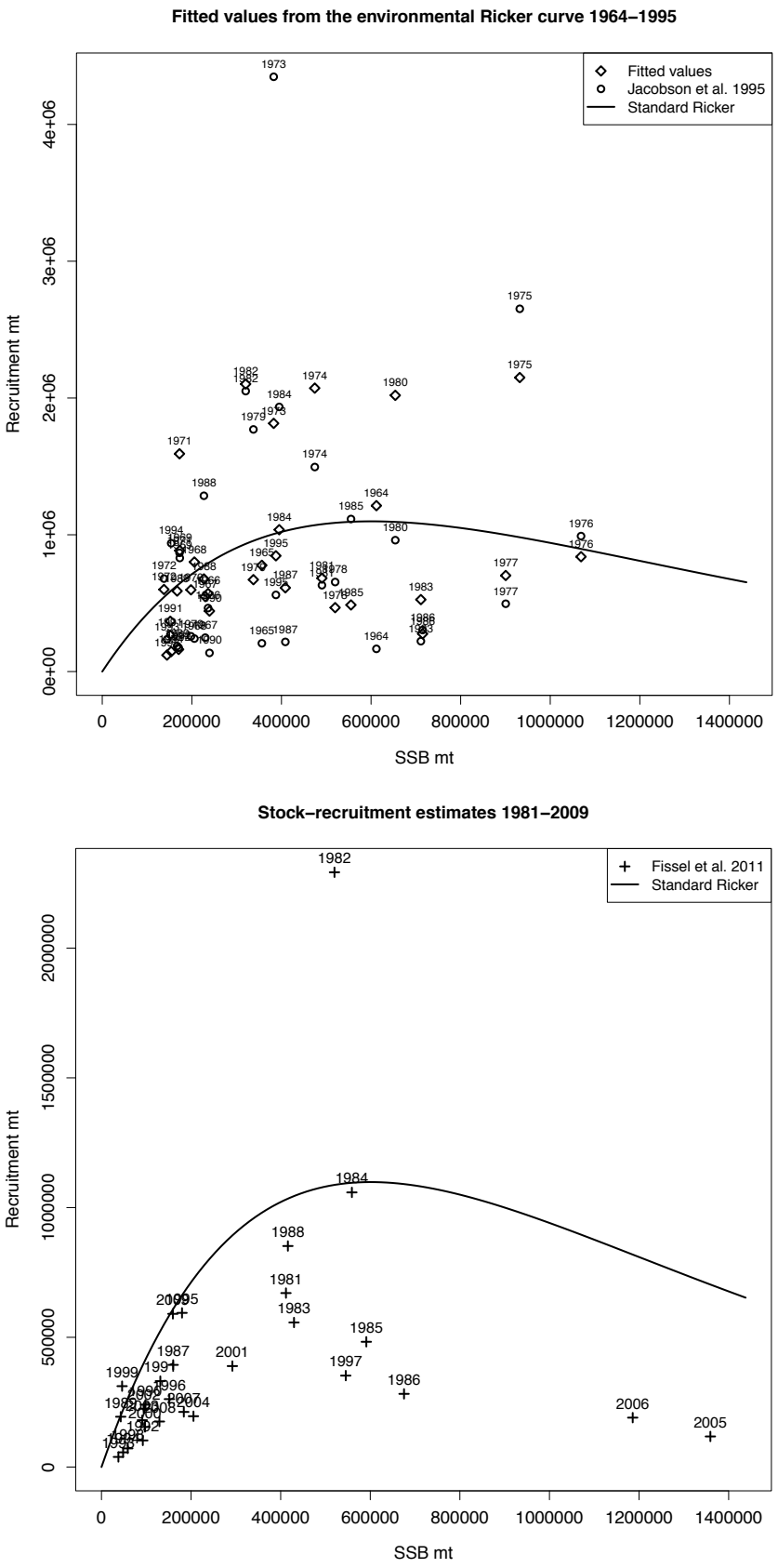

Figure 6. Fitted values of environmental Ricker model 1964–1995 (left panel) and predicted recruitment from the environmental Ricker curve 1981–2009 based on our $\widehat{SSB}_s$ (right panel).

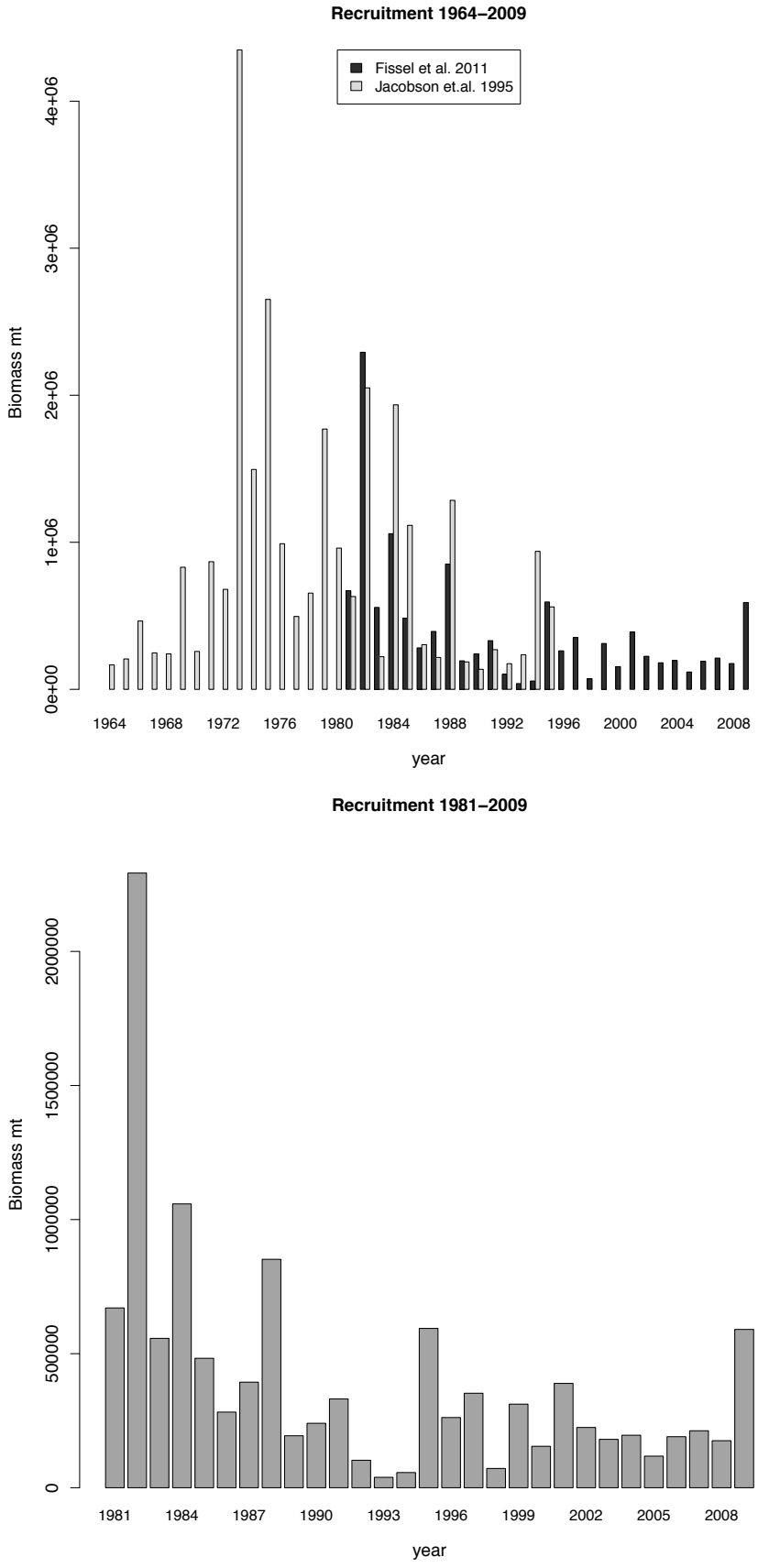

Figure 7. Comparison of historical and new annual recruitment (R_s) 1964–2009 (left panel). Annual recruitment 1981–2009 (right panel).

TABLE 5
AIC comparisons of the Ricker model specifications

AIC statistics				
Model	M^0 ($\rho_1 = \rho_2 = 0$)	M^T ($\rho_1 = 0, \rho_2 uc$)	M^W ($\rho_1 uc, \rho_2 = 0$)	M^{WT} ($\rho_1 uc, \rho_2 uc$)
AIC	93.5538	88.5827	87.5796	82.4666
Relative information likelihood statistics				
Model Comp.	$I(M^{WT}) \leq I(M^0)$	$I(M^T) \leq I(M^0)$	$I(M^W) \leq I(M^0)$	$I(M^{WT}) \leq I(M^w)$
Likelihood	0.0039	0.0833	0.0504	0.0776

Model M^0 is the standard Ricker null model, M^{WT} is the full environmental Ricker model, and M^W and M^T are models with only wind and temperature respectively. Likelihood ratios show relative information ($I(*)$) content. (*uc* means the coefficient was unconstrained).

The environmental factors were significant in the Ricker stock-recruitment model (fig. 6, table 4). The .05 quantile of the north-south wind stress anomaly was significant at the 0.1% level, and mean sea surface temperature anomaly at the 1% level. The contribution of the variables to explaining recruitment was further explored through an analysis of the AIC statisitics from different models (table 5). The unconstrained model M^{WT} had the lowest AIC. Models with only temperature (M^T) and only wind stress (M^W) were compared to the null model (M^0), the standard Ricker curve (section 2.4). The likelihood ratio statistic shows the contribution of the incorporating environmental information (table 5). The information gain in predicting recruitment provided by both environmental factors relative to the null model $I(M^{WT}) \leq I(M^0)$ is 0.004, below a 1% significance threshold. Temperature alone provides some improvement relative to the null model $I(M^T) \leq I(M^0)$ with a likelihood statistic of 0.08 which is below a 10% significance threshold, while a model with only wind stress $I(M^T) \leq I(M^0)$ is marginally above a 5% significance threshold with statistic of 0.05. The full model was compared to the model with only wind stress $I(M^{WT}) \leq I(M^w)$ and had a likelihood ratio statistic of 0.08 which is below a 10% level of significance. Both wind stress and temperature are significant in explaining recruitment, however wind stress has a comparatively larger influence. Both environmental variables were used in reported recruitment estimation (table 2). Graphical comparison of the standard Ricker and the environmental Ricker (fig. 6 left panel) shows that the temperture and wind stress produce improved fits for many years (e.g. 1975, 1977, 1982, and others), although this is not uniformly true for all years (e.g. 1976, 1980, and others).

The difference between the recruitment estimates and the standard Ricker curve shows the estimated influence of the environmental factors for 1981–2009 (fig. 6 right panel). Recruitment estimates above the standard Ricker line indicate favorable environmental conditions, while estimates below indicate the opposite. Many recent years, even when spawning biomass is high, fall below the standard Ricker curve. Comparison of Jacobson's historical data to ours show that the low recruitment levels are not without precedent and were observed in the mid to late '60s (fig. 7 left panel).

4 DISCUSSION

The anchovy ichthyoplankton data are not without their shortcomings. Previous anchovy assessments (Jacobson et al. 1995) used the *CB*, *CVT* and *PV* surveys with targeted adult and juvenile trawl surveys, and aerial spotter plane data. The latter two surveys are no longer conducted, hindering the calculation of a time-varying daily specific fecundity. Previous assessments also had staged eggs allowing the implementation of the DEPM and fundamental growth parameters had been recently estimated. While the precision of available parameters (Lo 1983) should be sufficiently accurate for HEPM estimation, parameters could hypothetically be time-varying and require updating to reflect the current environmental regime. Updated and extended sampling and research could provide further accuracy in future studies, but would not affect the trend in our estimates as these are driven by observed egg and larval densities.

The episodes of high egg densities, *SSB* and P_0 around 1997 and particularly in 2005 are prominent features of the data (fig. 3). Despite the periodic surges in spawning productivity we observed comparatively low larval densities (fig. 3). The low larval counts result in low corresponding estimates of the production at the time of hatching (P_h) which by the estimation procedure then translates into a high egg IMR. However, P_h is not directly observed and is estimated. Thus, the hatching transition itself has the potential to be a source of mortality, and one potentially susceptible to a variety of influences. Mortality at, or very shortly after, the time of hatching could confound egg IMR estimates. Regression discontinuity could be used to test this but would require staged eggs and thorough sampling to ensure accurate densities estimates around the hatching threshold.

Interpreted within the context of the modeling approach, the steady increase in the egg IMR is the primary cause of the low larval densities as opposed to the comparatively more stable coefficient of larval mortality (fig. 4). High mortality during the larval post-

yolk-sac consumption period, or critical period, would come through in mortality estimation as a lower (more negative) coefficient of larval mortality which does not appear in the data. Residual analysis does, however, show a slight negative residual bias in the later size classes that can be viewed as indicative of a critical period. The first feeding for anchovy larvae typically occurs at approximately 5mm (fig. B1 left panel). However, the magnitude of the residuals and the high egg IMR suggest post-yolk-sac stages are not the dominant source of mortality in anchovy ELH.

The assumption of a constant specific fecundity over time, used to estimate *SSB* (section 2.3), could bias estimates of *SSB*. Because anchovy are indeterminant spawners they will adjust their daily specific fecundity according to the environmental conditions: in high productivity years they will have a higher daily specific fecundity. The likely effect of our inability to capture this is overestimation of the spawning biomass in high egg productivity years (e.g. 2005–2006, fig. 5)[7]. Lacking data on spawning parameters it is unclear how to adjust the daily specific fecundity to account for temporal variation. Time trends and environmental factors in the specification of the daily specific fecundity were not significant. Despite our simplifying assumptions and inferior data, our estimates *SSB* fit the Jacobson et al. (1995) data quite well.

The failure of strong *SSB* to translate into strong *R* is analogous to the observation that high egg densities failed to translate into high larval densities. We observe higher pre-1989 larval densities and estimate strong pre-1989 recruitment classes. Larval densities after 1989 appear markedly smaller and correspondingly the environmental conditions estimate a lower recruitment through the environmental Ricker (fig. 6 right panel). The inclusion of environmental factors in the recruitment estimation was intended to provide insight into the potential sources of larval mortality by estimating a reduced form relationship between *SSB* and *R*. The time between spawning and recruitment spans the egg and larval phases of development. These phases of development are thought to be when pre-recruitment mortality is greatest. Motivated by Peterman and Bradford (1987), who examined the impact of wind speed exceeding a threshold on larval survival and hence recruitment, we use the 5% quantile of the north-south wind stress anomaly to capture this. Cooler temperatures are thought to allow for the fuller development of anchovy larvae; as such we use the mean temperature anomaly. The environmental variables are incorporated into the regression in a straightforward fashion as exponential terms.

The reduced form approach to examining environmental influences employed in this paper does not identify the point during the development process that these factors (or factors for which they're proxying) are influencing mortality. Nonetheless, one can interpret environmental Ricker as a linear model for the growth rate and carrying capacity. Equation 5 can be algebraically manipulated to express the growth rate as $\log(A) + \rho^* x$ where x is vector of environmental factors[8]. If one interprets the growth rate as an aggregate index of potential, then survival/mortality is a component of this index and the environmental Ricker serves as a model for the influence of environmental factors on ELH mortality. Stock-recruitment modeling, in general, cannot single out specific ELH stage(s) that the environmental factors influence, nor can it provide the direct linkage to the physiological mechanism impacting mortality. However, these mechanisms may be complex, nonlinear and difficult to model parametrically on a small scale. The environmental Ricker can be viewed as testing the association between the aggregate ELH mortality impact on growth rates and the environment. The utility of this interpretation clearly depends on one's perspective regarding stock-recruitment growth rates and ELH mortality. The significance of wind stress in particular (table 4) coupled with the biological research of Peterman and Bradford (1987) on larval survival support the straight forward incorporation of environmental factors in Ricker model as useful method for potentially capturing some environmental influences on ELH mortality.

Recruitment estimates indicated that the strong years of productivity (e.g. 1997 and 2005, 2006) did not translate into large recruitment classes due to poor environmental conditions. Warmer than normal sea surface temperatures and unfavorable wind patterns have contributed to poor recruitment. However, the vast majority of changes in mortality for the egg through 9.25 mm larval class appears to have occurred during the egg phase. Temperature is a potential cause of the increasing egg IMR; however, were temperature a significant contributor one would think it should be a stronger predictor of recruitment. Other potential explanations for the increasing egg IMR could be conceived, such as an increased abundance of euphausiids that can prey on the stationary eggs more easily than the mobile mature larvae. Exploration of hypotheses such as this are left for future research. Also, stock-recruitment modeling may not be ideal for identifying factors influencing the egg IMR, as large variation in the late larval and juvenile phases may leave a strong signature on recruitment, masking the straightforward identification of environmental influences on egg mortality. Ultimately, we are

[7]Daily specfic fecundity is $1/\gamma$, so underestimating fecundity results in overestimation of *SSB*, $SSB = P_0{}^*\gamma$.

[8]The Ricker model $R = SSB^* e^{r(1+SSB/K)}$ has growth rate r and carrying capacity K. Let x be a vector of environmental factors. Rewrite Equation 5 as $A^*SSB^* e^{B^*SSB + \rho^* x} = SSB^* e^{(\log(A)+\rho^* x)(1+(B/(\log(A)+\rho^* x))SSB)}$. By analogy, the environmental Ricker has growth rate $r = \log(A) + \rho^* x$ and capacity $K = (\log(A) + \rho^* x)/B$.

currently unable to explain through biological or environmental reasons the increases in the egg IMR.

While this paper does not give an overall estimate of the stock size, prolonged regimes of low productivity and recruitment combined with the short life spans of anchovy will eventually translate into a lower overall stock size. Given that the regime of low productivity has persisted for fifteen plus years, there is reason to believe that the northern anchovy stock as a whole is not as large and strong as it once was in its heyday of the '80s or even the mid '90s, and impacts on the stock and potentially the ecosystem may be at risk if a large fishery for anchovy develops. Recognizing the global demand for small pelagic fish is strong and that U.S. landings in the anchovy fishery have been on the increase (PFMC 2010), additional attention, sampling, and research into the anchovy fishery would be prudent.

5 IMPROVING FUTURE ANALYSIS

Our analysis was based on the best available data and well-established methods for estimating key population parameter. However, there are shortcomings which are not defects in the analysis, but rather directions for future research and data collection. We highlight these issues so that they may be considered for improving future anchovy stock assessments.

- Unstaged eggs preclude the use of the more accurate DEPM. The staging of anchovy eggs would provide data on egg production-at-age which could be used to model the egg mortality curve and provide more precise estimates of egg production and the IMR (Lo 1985b).
- Parameter estimates obtained from the literature (e.g. aging, see appendix A2), were estimated around 1985 and may require updating. It's possible that parameter values could have changed over time.
- Because no trawl surveys were undertaken, we had to assume constant stock parameters to infer spawning stock biomass. Targeted trawl sampling of the anchovy stock would enable the estimation of a time-varying daily specific fecundity.
- The methods used here were developed twenty years ago. More complex Bayesian hierarchical models (BHM) might be considered, enabling one to utilize data from other years (Clark 2007). Research into developing up-to-date statistical methods for anchovy that explicitly account for the various stages of estimation could improve estimation precision.

A sampling scheme tailored for the range of northern anchovy and updated parameters and methods would improve the accuracy of estimation but would not substantially affect the trends in the data or the conclusions. Despite these areas where improvements are needed, the results provided in this paper accurately reflect trends in the status of the central subpopulation of northern anchovy.

6 ACKNOWLEDGMENTS

We thank Ed Weber for providing the data; participants at the CalCOFI conference 2010 for their many helpful comments; Kevin Hill; John Field; and reviewers for insightful comments on earlier versions of this paper. The findings and conclusions in the paper are those of the authors and do not necessarily represent the views of the National Marine Fisheries Service.

LITERATURE CITED

Aydin, K. 2005. Fisheries and the Environment: Ecosystem Indicators for the North Pacific and Their Implications for Stock Assessment. NMFS AFSC Proceeds of the First Annual Meeting of the National Marine Fisheries Service's Ecological Indicators Research Program.

Butler, J. 1989. Growth during the larval and juvenile stages of the northern anchovy in the California Current during 1980–84. Fishery Bulletin. 87:645–652.

Burnham, K. P. and D. R. Anderson. 2002. Model Selection and Multimodel Inference: A Practical Information-Theoretic Approach. Springer Verlag.

CalCOFI Net Descriptions. 2010. Description of Nets Cal1MOBL (C1), CalBOBL (CB), CalVET (CVT), PairOVET (PV). http://swfsc.noaa.gov/textblock.aspx?Division=FRD&ParentMenuId=213&id=1376. Accessed 08–23–2010.

Clark. J. S. 2007. Models for Ecological data, an Introduction. Princeton University Press. 817pp.

Eber, L. E. and R. P. Hewitt. 1979. Conversion Algorithms of the CalCOFI Station Grid. Calif. Coop. Oceanic Fish Invest. Rep. 20:135–137.

Fiedler, P., R. D. Methot, and R. P. Hewitt. 1986. Effects of California El Niño 1982–1984 on the northern anchovy. Journal of Marine Research. 44:317–338.

Hewitt, R. P. 1981. The Value of Pattern in the Distribution of Young Fish. Rapp. P.-v. Reun. Cons. Int. Explorer. Mer. 178:229–245.

Hewitt, R. P. and R. D. Methot. 1982. Distribution and Mortality of Northern Anchovy Larvae in 1978 and 1979. Calif. Coop. Oceanic Fish Invest. Rep. 23:226–137.

Hewitt, R. P. and G. D. Brewer. 1983. Nearshore Production of Young Anchovy. Calif. Coop. Oceanic Fish Invest. Rep. 24:235–244.

Hewitt, R. P. 1985. Comparison between Egg Production Methods and Larval Census Method for Fish Biomass Assessment. An egg production method for estimating spawning biomass of pelagic fish: application to the northern anchovy, *Engraulis mordax*. US Dep. Commer., NOAA Tech. Rep. NMFS. 36:95–99.

Hushby, D. and C. Nelson. 1982. Turbulence and vertical stability in the California Current. Calif. Coop. Oceanic Fish Invest. Rep. 23:113–129.

Hunter, J. R. and B. J. Macewicz. 1985. Measurement of spawning frequency in multiple spawning fishes. Lakser ed. NOAA Technical Report NMFS. 36(iii):79–94.

Jacobson, L. D., N. C. H. Lo, S. F. Jr. Herrick, and T. Bishop. 1995. Spawning Stock Biomass of the Northern Anchovy in 1995 and Status of the Coastal Pelagic Fishery During 1994. Administrative Report LJ-95-11. NMFS.

Jacobson, L. D., N. C. H. Lo, and J. T. Barnes. 1994. A biomass-based assessment model for northern anchovy, *Engraulis mordax*. Fishery Bulletin. 92(4):711–724.

Lasker, R. 1981. Factors contributing to variable recruitment of the northern anchovy in the California current: contrasting years, 1975–1978. Rapp. P.-v. Reun. Cons. Int. Explorer. Mer. 178:375–388.

Lasker, R. 1985. An egg production method for estimating spawning biomass of pelagic fish: application to the Northern Anchovy, *Engraulis mordax*. NOAA Technical Report NMFS. 36(iii):1–99.

Lo, N. C. H. 1983. Re-estimation of three parameters associated with anchovy egg and larval abundance: temperature dependent incubation time, yolk-sac growth rate and egg and larval retention in mesh nets. NOAA Technical Memorandum NMFS. NOAA-TM-NMFS-SWFC-33:1–33.

Lo, N. C. H. 1985a. Egg production of the central stock of northern anchovy, *Engraulis mordax*, 1951–1982. Fishery Bulletin, 83:137–150.

Lo, N. C. H. 1985b. A model for temperature-dependent northern anchovy egg development and an automated procedure for the assignment of age to staged eggs. An egg production method for estimating spawning biomass of pelagic fish: application to the northern anchovy, *Engraulis mordax*. US Dep. Commer., NOAA Tech. Rep. NMFS. 36:43–50.

Lo, N. C. H. 1985c. Modeling life-stage-specific instantaneous mortality rates, an application to northern anchovy, *Engraulis mordax*, eggs and larvae. Fishery Bulletin. 84:395–407.

Lo, N. C. H., B.J. Macewicz, D.A. Griffith, and R.L. Charter. 2008. Spawning biomass of Pacific sardine (*Sardinops sagax*) off U.S. in 2008. NOAA Technical Memorandum NMFS. 430:1–33.

MacKinnon, J. G. 2006. Bootstrapping methods in econometrics. The Economic Record. 82:S2–S18.

Methot, R. D. and R. P. Hewitt. 1980. A Generalized Growth Curve For Young Anchovy Larvae: Derivation and Tabular Example. Administrative Report LJ-80-17, NMFS.

PFMC. 1978. 1983. Northern anchovy fishery management plan. PFMC, Portland, OR. Federal Register 43(141):31655–31783. PFMC Amendment 5 to the Northern anchovy fishery management plan: Incorporating the final supplementary EIS/DRIR/IRFA. PFMC, Portland, OR.

PFMC 2010. Status of the Pacific Coast Coastal Pelagic Species Fishery and Recommended Acceptable Biological Catches: Stock Assessment and Fishery Evaluation. PFMC, Portland, OR.

Peterman, R. and M. Bradford. 1987. Wind speed and mortality rate of marine fish: northern anchovy. Science. 235:354–365.

Ricker, W. E. 1954. Stock and Recruitment. Fisheries Research Board of Canada.

Rykaczewski, R. and D. Checkley. 2008. Influence of ocean winds on the pelagic ecosystem in upwelling regions. Proceedings of the National Academy of Sciences. 105:1965–1970.

Smith, P. E. and S. L. Richardson. 1977. Standard techniques for pelagic fish eggs and larval survey. FAO Fisheries Techniques Paper. 175:27–73.

Weber, E. and S. McClatchie. 2009. rcalcofi: Analysis and Visualization of CalCOFI Data in R. Calif. Coop. Oceanic Fish Invest. Rep. 50:178–185.

Zweifel, J. and R. Lasker. 1976. Prehatch and posthatch growth of fishes: a general model. Fisheries Bulletin. 74:609–621.

Zweifel, J. and P. E. Smith. 1981. Estimates of Abundance and Mortality of Larval Anchovies (1951–75): Application of a New Method. Rapp. P.-v. Reun. Cons. Int. Explorer. Mer. 178:284–259.

APPENDIX A: METHODS FOR DENSITY CALCULATIONS AND AGING

A1 EGG AND LARVAE DENSITY CORRECTIONS

Assignment into larval size classes was necessary prior to adjusting for extrusion and avoidance as the likelihood of extrusion decreases with length but avoidance increases with age (which is an increasing function of length). Sorting is based on preserved larval size which is recorded at the time of staging. Length thresholds for the larval size classes (Lo 1985a) are listed in table A1. Because of differences in mesh sizes of the nets, *CVT/PV* and *CB* nets differ in their sampling efficiency. Smaller larvae and eggs are more likely to extrude through the *CB* net, but are retained more efficiently in the finer mesh size of the *CVT/PV*. However, *CB* is more efficient at catching larger larvae. Extrusion factors (table A1), calculated by Lo (1983) to compensate for these differences, were applied to the size classes to obtain extrusion free counts (0.075 mm mesh was treated as extrusion free (Lo 1983)).

Avoidance corrections were made to *CB* samples to correct for the propensity for older developed larvae to avoid the net. No avoidance corrections are necessary for *CVT/PV* because the net is pulled vertically through the water column. The avoidance equation from Lo et al. (1989) was used for the correction:

$$avd_c = \frac{1 + DNl_c}{2} + \frac{1 - DNl_c}{2} * cos(2\pi * hr/24) \quad (1)$$

where *hr* is the time of day on a 24 hour clock the tow was taken, and DNl_c represents the day/night catch ratio for larval size class *c*. The DNl_c used here differs from the one used in Lo et al. (1989). In contrast to Lo et al. (1989) we calclated DNl_c as $DNl_c = e^{-0.229*c}$ because it is more up-to-date and logically consistent.

Raw egg and larval counts were standardized to an area-density using standard haul factors (*SHF*) (Kramer et al. 1972); where *SHF* = 10*(tow depth/volume of water filtered) which represents abundance beneath an area of 10 m^2 integrated over the depth of the tow. This 10 m^2 area-density will be refered to simply as a 10 m^2 density. A second adjustment was made for the percentage of total plankton volume sorted from the samples. The overall adjustment can be represented as $rct_k * shf_k / prst_k$ where rct_k is the raw count (egg or larval), $prst_k$ is the percentage sorted and shf_k is the *SHF* for sample k[1].

TABLE A1
Larval size classes and length ranges, extrusion correction factors for bongo (CB), calvet and pairovet (CVT/PV) and growth curve coefficients.

Size Class	Range [a]	*CB*[b]	*CVT/PV*[c]	Month	a^{mm} [d]
eggs	N/A	12.76	1.10	Jan.	0.046
2.5	[2,3.25]	6.08	1.46	Feb.	0.048
3.75	[3.25,4.25]	2.58	1.37	March	0.05
4.75	[4.25,5.25]	1.62	1.30	April	0.052
5.75	[5.25,6.25]	1.24	1.25		
6.75	[6.25,7.25]	1.10	1.21		
7.75	[7.25,8.25]	1.00	1.00		
8.75	[8.25,9.25]	1.00	1.00		
9.75	[9.25,10.25]	1.00	1.00		

[a]Assignment to classes is based on preserved larval lengths (section 2.2.2). All larval sizes are measured in mm.
[b]Extrusion factors for *CB* computed directly from the logistic model of Lo (1983) equation (6), table 4.
[c]Extrusion factors for *CVT* and *PV* are fitted values of a logistic regression on the raw estimates from Lo (1983).
[d]Gompertz growth second stage parameter (Methot and Hewitt 1980).

A2 EGG INCUBATION TIME AND AGING OF LARVAE

Unstaged egg data precluded us from aging individual or even groups of eggs, however, the incubation time has a known temperature dependent functional from Lo (1983). Missing temperature data from the surveys were rare; occurances were interpolated using an inverse distance spatially weighted average of other observed temperatures during that cruise. Temperature measurements at each sample, *k*, were used in the relationship specified by Lo (1983) to calculate incubation times:

$$t_k^I = 18.726 * e^{-0.125 * tmp_k} \quad (2)$$

where t_k^I is the incubation time and tmp_k is the temperature measured in degrees Celsius.

The calculation of larvae age requires the live larval length. Preserving agents used at the time of sampling and tow time can shrink larvae. Therefore adjustments for these factors were made before aging using the correction function specified in Theilaker (1980):

$$l_k = \log(ff * pls_k) + 0.289 * \exp(-0.434 * ff * pls_k * q^{-0.68}) \quad (3)$$

where l_k is the estimated length of live larvae in millimeters (mm) from sample *k* with a preserved larval length of pls_k mm, a tow time of *q* minutes, and *ff* is a paramter base on the preserving agent. Formalin was the preserving agent so *ff* = 1.03 (Theilaker 1980). Tow time was not included in our data set and was assumed to be 15.5 minutes based on CalCOFI sampling guidelines (Cal-

[1]Sample indices *k* are specific to a year, cruise, and station. Furthermore, occasionally multiple samples were observed at a station on a cruise, each would have its own index *k*. Without loss of generality, a single index is used here, and later, as explicitly specifying all dimensions of the indices would provide no further insight.

COFI 2010). The remaining numeric values were taken from Theilaker (1980). No rounding of *pls* by grouping into size classes was carried out prior to estimation of *l* and *pls* was recorded up to the precision of 0.1 mm in our data set.

Larvae were aged using a two-stage Gompertz growth curve (GGC). This approach was first proposed for the use on anchovy larvae by Methot and Hewitt (1980) and later with updated first-stage parameter estimates by Lo (1983). The first stage of the GGC accounts for growth through yolk-sac consumption, which is approximately the first two size classes 2.5 mm and 3.75 mm. Aging during the first stage of the GGC is temperature dependent while aging during the second stage is month-of-sampling dependent. Because of this, it is necessary to compute ages as sample specific. The first stage of the GGC is specified as:

$$T1(l_k) = \left(\frac{-1}{a_k^{tmp}}\right) * \log\left(\frac{\log(l_k/4.25)}{\log(0.32/4.25)}\right) \text{ for } l_k \le 4.1 \text{ mm}$$

$$a_k^{temp} = 0.1108 * e^{0.1173 * tmp_k} \quad (4)$$

where $T1(l_k)$ is the estimated age of larvae with length l_k (equation A3). The value 4.25 controls the upper bound of the growth curve (mm) during the first stage of growth while the value 0.32 is the hypothetical minimum larval size. The temperature dependent parameter a_k^{tmp} was specified by Lo (1983). The second stage of the GGC is meant to capture the post yolk-sac consumption period of larval growth, and is specified as:

$$T2(l_k) = \left(\frac{-1}{a^{mn}}\right) * \log\left(\frac{\log(l_k/27)}{\log(4.1/27)}\right) \text{ for } 4.1 \text{ mm} < l_k < 27 \text{ mm} \quad (5)$$

where $T2(l_k)$ is the age of larvae length l_k (from equation A3) since the first stage. The value 27 controls the upper bound of the second-stage GGC and 4.1 is the length at which larvae transition into the second stage of growth. The monthly parameter α^{mn} was estimated by Methot and Hewitt (1980) and its values are listed in table A1. The total age of the larvae is $t(l_k) = T1(l_k)$ for yolk-sac larvae which haven't entered the second stage of growth ($l_k \le 4.1$ mm) and $t(l_k) = T1(4.1) + T2(l_k)$ for larvae beyond the yolk-sac stage ($l_k > 4.1$ mm)[2].

A3 DAILY LARVAL PRODUCTION

Even with regularly scheduled ichtyoplankton surveys the number of eggs or larvae from a single sample on a given cruise at a station is too few to accurately characterize densities. To minimize small sample biases, aggregation over cruises was necessary prior to the calculation of production statistics and mortality estimation. Each sample tow was assigned to a CalCOFI station (Weber and McClatchie 2009; Eber and Hewitt 1979) and multiple samples observed at a station on a cruise were averaged. No weighting of cruises was used and all data were averaged across cruises occuring during January through April of a year to obtain annual station specific data. A final average over stations was needed to obtain accurate annual mortality curve estimates for the region as a whole.

The production of larvae in a size class per day per unit area, *DLP*, is estimated as standing stock of larvae in a size class over the days that larvae spend in that class, or duration. Duration is the difference between the ages (equations 4 and 5) at the size class break points (table A1). Let $n_{c,s}$ be the standing stock of larvae[3] and $d_{c,s}$ be the duration of size class *c* in year *s*. *DLP* is then calculated as $dlp_{c,s} = n_{c,s}/d_{c,s}$. Avoidance by larvae older than twenty days (Lo 1985a) biases estimates of *DLP*. Larvae were found to have reached an age of twenty days towards the end or just after the 9.75 mm size class. To mitigate these biases we omitted class sizes larger than 9.75 mm from the analysis.

[2]Frequently, age will be referred to simply as *t*, and the functional dependence of age on length $t(l_k)$ being explicit only where needed.

[3]The standing stock of larvae is the total corrected count of all larvae in a size class and can be viewed as the integral over ages in that size class, e.g. $n_{c=3.75\text{ mm}} = P_h \int_{t(l=3.25\text{ mm})}^{t(l=4.25\text{ mm})} \left(x/t^l\right)^{-\beta}\, dx$.

APPENDIX A LITERATURE CITED

Eber, L. E. and R. P. Hewitt. 1979. Conversion Algorithms of the CalCOFI Station Grid. Calif. Coop. Oceanic Fish Invest. Rep. 20:135–137.

Kramer, D., M. Kalin, G. Stevens, J. R. Thrailkill, J. R. Zweifel. 1972. Collecting and processing data on fish eggs and larve in the California Current Region. NOAA Tech. Rep. NMFS Circ.370:38.

Lo, N. C. H. 1983. Re-estimation of three parameters associated with anchovy egg and larval abundance : temperature dependent incubation time, yolk-sac growth rate and egg and larval retention in mesh nets. NOAA Technical Memorandum National Marine Fisheries Services. NOAA-TM-NMFS-SWFC-33:1–33.

Lo, N. C. H. 1985a. Egg production of the central stock of northern anchovy, *Engraulis mordax,* 1951–1982. Fishery Bulletin, 83:137–150.

Lo, N. C. H., J. R. Hunter, and R. P. Hewitt. 1989. Precision and bias of estimates of larval mortality. Fishery Bulletin, 87(3):399-416.

Methot, R. and R. P. Hewitt. 1980. A Generalized Growth Curve For Young Anchovy Larvae: Derivation and Tabular Example. Administrative Report LJ-80-17, National Marine Fisheries Services.

Theilacker, G. H. 1980. Changes in body measurements of larval northern anchovy, *Engraulis mordax*, and other fishes due to handling and preservation. Fishery Bulletin. 78(3):685–692.

APPENDIX B: BOOTSTRAPPING MORTALITY PARAMETERS

B1 INTRODUCTION

This appendix explains the bootstrapping methods used to estimate the annual variability of the early life-history parameters: production at the time of hatching (P_h), the coefficient of larval mortality (β), egg instantaneous mortality (IMR) (α) and the daily egg production (P_0). Mortality curves estimated in the main manuscript (section 2.2.1), used a Pareto type mortality curve (this regression will be referred to as MC^0). The iterative procedure used to identify the egg IMR (α) (equation 2) and the calculation of P_0 (equation 3) yields only point estimates for α and P_0. Lo (1985a) approached the problem of estimating variability for these point estimates using an approximation based on the delta method. When applied to our data the standard errors produced were too large to be meaningful, frequently displaying a coefficient of variation greater than 1.

The bootstrap is used to provide more precise estimates of the variability using confidence intervals of the bootstrapped distributions. An advantage of this approach is that it characterizes confidence intervals for a general class of true underlying distributions, in particular accurate interval construction is more robust to fat tails and extreme tail events. The residual bootstrap method (MacKinnon 2006) is used, which samples from the residual empirical cumulative distribution function (cdf) of MC^0 and applies the resampled residuals to the fitted daily larval production estimates $\widehat{dlp}$ to for bootstrapped $\widehat{dlp}^*$, on which new mortality curves with new parameters were estimated. Normalization is required to stabilize the heteroskedasticity in the residual distribution. When applied to equations 1–3 annual bootstrap distribution of β, P_h, α, and P_0 are created from which we take the 0.025 and 0.975 quantiles as the 95% confidence interval of the associated statistics.

The results of methods used in this appendix are 95% confidence intervals for β, P_h, α, and P_0. In addition, the residual analysis necessary for the heteroskedasticity stabilization is discussed in the results and discussion section.

The next section describes the bootstrapping methods in detail. Section three reports some of the intermediate estimation results and section four discusses the methods used and the residual distribution. Confidence intervals were referenced in the text of the main manuscript and can be found in table 1, and figure 4.

B2 METHODS

The residual bootstrap uses the empirical cdf of the residuals from the initial estimation of the mortality curve MC^0 (section 2.2.1) as a measure of the true error term associated with larval mortality estimation. Residuals are given by

$$\widehat{\varepsilon_{c,s}} = dlp_{c,s} - \widehat{dlp_{c,s}}, \text{ where } \widehat{dlp_{c,s}} = \widehat{P_{h,s}} \left({t_{c,s}}/{t_s^I} \right)^{-\widehat{\beta_s}} \quad \text{(B1)}$$

and $\widehat{\beta_s}$ and $\widehat{P_{h,s}}$ are the annual (s = 1981, 1982, …, 2009) estimated parameter values relating daily larval production ($dlp_{c,s}$) to larval ages ($t_{c,s}$) over the incubation time (t_s^I) for larval size class (c $\in$ {*larval class* 2.5 mm, 3.75 mm, …, 9.75 mm}) (appendix A1 and table A1).

There were eight larval size classes in a year and simply resampling from the eight residuals on that year would not provide a sufficiently rich set of residuals to characterize the true residual distribution. Furthermore, size class dependent heteroskedasticity precluded resampling from this small set of residual. To overcome this residuals from all 29 years of mortality estimation normalized by exploiting the longitudinal structure were of the residual data. Linear approaches to bootstrap normalization are not applicable for nonlinear regression (MacKinnon 2006)[1]. We use a linear regression with ages and years as independent variables to model the heteroskedasticity and purge the residuals of class and temporal dependence. Higher-order polynomial terms and other categorical variables were tried, and a first-order linear regression minimized the AIC criterion. The heteroskedasticity stabilizing regression is:

$$\omega_{c,s} = |\widehat{\varepsilon_{c,s}}|, \quad \gamma_s = \frac{s - mean(s)}{stdev(s)}$$

$$\omega_{c,s} = \theta_0 + \theta_1 t_{c,s} + \theta_2 \gamma_s + \theta_3 D2_s + \nu_{c,s} \quad \text{(B2)}$$

where $\omega_{c,s}$ is the absolute deviation of the residual, γ_s is the normalized year, $t_{c,s}$ is the larval size class age, $D2_s$ is a categorical 0–1 variable capturing the anomalous years 2005 and 2006 ($D2_s$ = 1) (section 2.3) and $\nu_{c,s}$ is the error term. Outliers exerted excessive leverage and led to a poor fit. Outliers were determined from a preliminary regression of B2 as observations associated with a preliminary residual z-score greater than six, $6 \leq {\widehat{\nu}_{c,s} - mean_{0.01}(\widehat{\nu})}/{stdev_{0.01}(\widehat{\nu})}$ (where the 0.01 subscript indicates a trimmed mean/standard deviation). This identified three observations as outliers. Equation B2 was then fit with outliers removed to determine the final fit. The fitted root-squared residuals were then used to normalize the residuals distribution.

[1] E.g. using the diagonal element of the hat data matrix $X(X'X)X'$ where X is the data matrix used in liear regression.

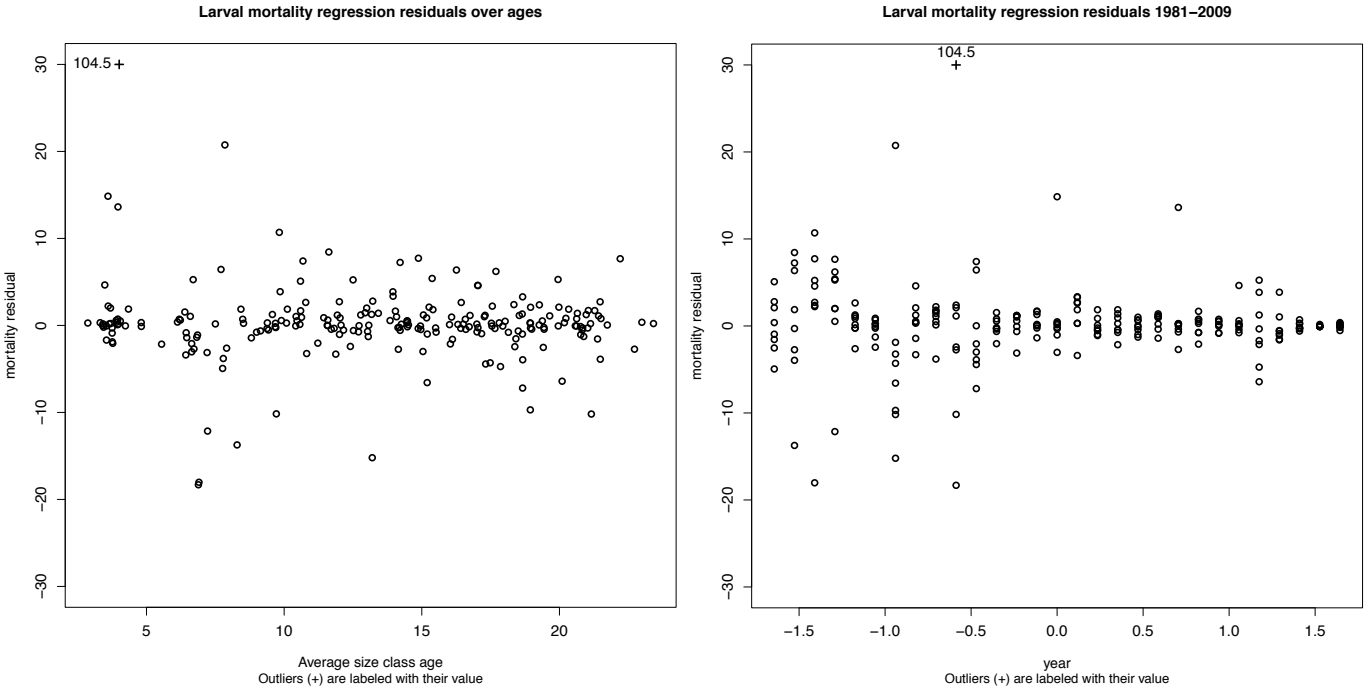

Figure B1. Larval mortality residuals (from equation 1) over the average size-class ages ($t_{c,s}$) (left panel), and normalized years (y_s) (right panel) 1981–2009.

$$\widetilde{\varepsilon_{c,s}} = \varepsilon_{c,s} \Big/ |\widehat{\omega_{c,s}}| \tag{B3}$$

where

$$\widehat{\omega_{c,s}} = \hat{\theta}_0 + \hat{\theta}_1 t_{c,s} + \hat{\theta}_2 \gamma_s + \hat{\theta}_3 D2_s \tag{B4}$$

This procedure produces a set (29 years x 8 classes = 232) of temporally and class "independent" residuals forming a distribution that was used to perform the bootstrapped. For each year s, eight residuals (one for each size class) were randomly sampled with replacement from the set of residual, $\varepsilon^{BS} \in \{\widetilde{\varepsilon_{c,s}}\}$. Residuals were centered and rescaled to the have the size class and temporal variance as determined by equation B4. The new resampled residuals were added to the fitted daily larval production from the initial estimation stage (equation 1 and B1) to obtain bootstrapped *DLP* estimates.

$$\varepsilon^{BS\prime} = \varepsilon^{BS} - \frac{1}{8}\sum_{i=1}^{8} \varepsilon_i^{BS},\ \varepsilon_{c,s}^{*} = \varepsilon^{BS\prime} * |\widehat{\omega_{c,s}}|,$$

$$\text{and } dlp_{c,s}^{*} = \widehat{dlp_{c,s}} + \varepsilon_{c,s}^{*} \tag{B5}$$

The bootstrapped *DLP* $dlp_{c,s}^{*}$ estimates were then used to fit a new mortality curve.

$$dlp_{c,s}{}^{*} = \widehat{P_{h,s}}^{*} \left(t_{c,s} \Big/ t_s^I \right)^{\widehat{-\beta_s}^{*}} \tag{B6}$$

The estimated production at the time of hatching $\widehat{P_{h,s}}^{*}$ was then used with the standing stock of eggs (m_s) and the incubation time (t_s^I) to determine the egg IMR ($\hat{\alpha}_s^{*}$) by iterative method (section 2.2.1, equation 2).

$$\hat{\alpha}_s^{*} \text{ is the } \alpha_s \text{ such that } \frac{m_s}{\widehat{P_{h,s}}^{*}} = \frac{e^{\alpha_s * t_s^I} - 1}{\alpha_s} \tag{B7}$$

Bootstrapped $\widehat{P_{0,s}}^{*}$ was obtained by the calculation (section 2.2.1, equation 3):

$$\widehat{P_{0,s}}^{*} = \widehat{P_{h,s}}^{*} e^{\widehat{\alpha_s}^{*} * t^I} \tag{B8}$$

The preceding bootstrap algorithm (equations B1–B6) was repeated 1000 times. On occasion, some of the bootstrap residuals ($\varepsilon_{c,s}^{*}$) would be sufficiently negative to produce a daily larval production value less than zero ($dlp_{c,s}^{*} < 0$) which was treated as if no larvae were observed for that class. If this happened for more than two size classes during an iteration then that iteration was discarded and repeated. If NLS failed to converge or β_s was estimated to be positive (illogical curvature of the mortality curve) or $\beta_s < -3$ (suggesting convergence in a bad area of the parameter space) then a log linearization was performed and parameters were estimated using OLS. Final estimates of $P_{h,s}$ were then calculated assuming normality of $\log(P_{h,s})$ (i.e. $P_{h,s}$ is log normally distributed).

This algorithm produced bootstrap distributions ($\{\widehat{\beta_s}^{*}\}$, $\{\widehat{P_{h,s}}^{*}\}$, $\{\widehat{\alpha_s}^{*}\}$, $\{\widehat{P_{0,s}}^{*}\}$) each with 1000 observations. The 0.025 and 0.975 quantiles of these distri-

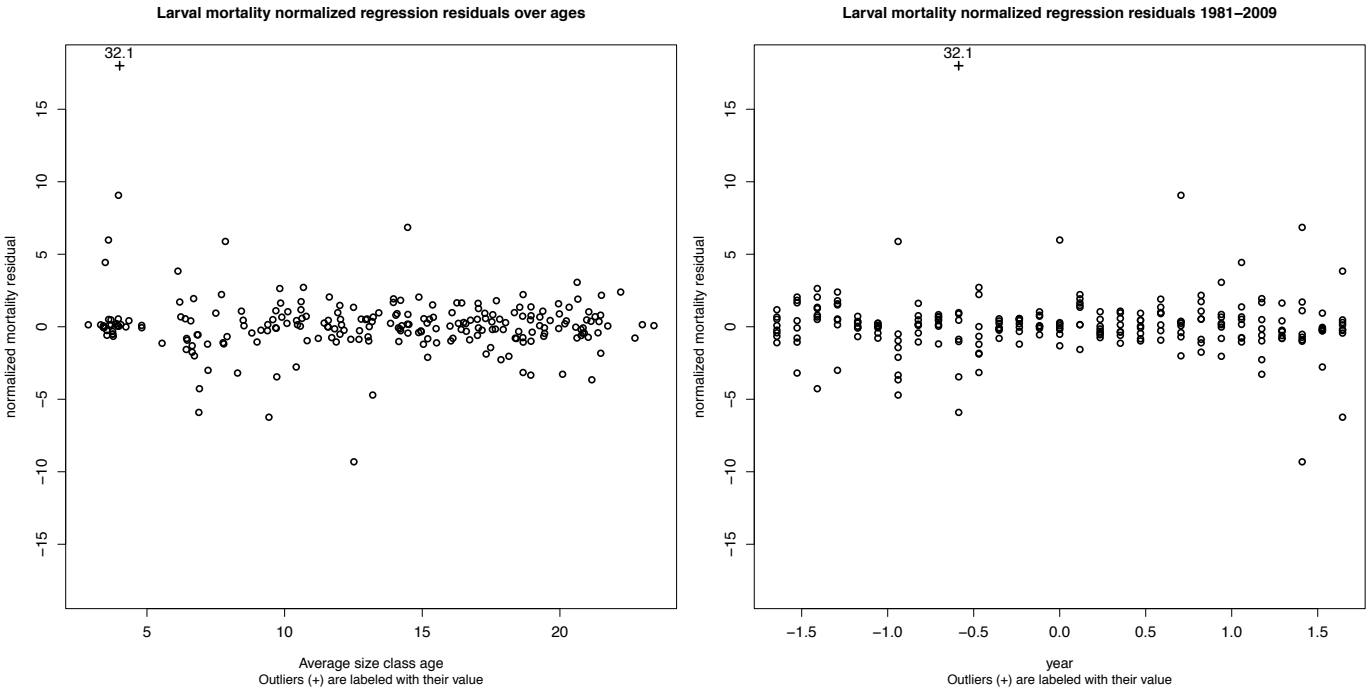

Figure B2. Larval mortality residuals over average size-class ages from hatching ($t_{c,s}$) (left panel), and normalized years (y_s) (right panel) after normalization.

butions were taken as a nonparametric estimate of their respective 95% confidence intervals.

B3 RESULTS

The residuals from MC^0 (section 2.2.1, equation 1) displayed heteroskedasticity across both ages and years (fig. B1). Coefficient estimates for the heteroskedasticity stabilizing regression support the visual observation of a decreasing volatility with both age and time (table B1).

Based on the observed heteroskedasticity in the residuals, failing to stabilize the class and temporally dependent variation would introduce spurious nonstationarity into the residuals upon resampling for the bootstrap. The heteroskedasticity stabilizing regression (equation B2) does an acceptable job of modeling the heteroskedasticity in MC^0 (table B1). Graphical analysis shows that dispersion around the mean is more evenly distributed (fig. B2) after the variance stabilization. Outliers are still outliers in the normalized residuals as they were intentionally removed during the regression. The normalized residual distribution is still highly leptokurtotic even with the outliers removed with a kurtosis of 12.08 (a standard normal distribution has a kurtosis of 3). Thus, heavy tails and extreme tail events are still a feature of the residual distribution used for resampling.

The grid search algorithm over initial condition during the NLS estimation (section 2.23) made more iterations computationally prohibitive in R. Furthermore, it was verified through histograms of 1000 iterations per-year that the number of iterations was sufficient. Marginal increases in the number of iterations to 1500 and 2000 iteration failed to noticeably change the distribution or confidence intervals from it.

Bootstrapped confidence intervals were referenced in the text of the main manuscript and can be found in table 1, and figure 4.

B4 DISCUSSION

Residual bootstrapping treats the empirical distribution formed by the set of residuals as sufficient for the true distribution. Resampling randomly reassigns residual from other classes and times to the fitted *dlp* estimates. Failing to account for the class and temporal differences in the residual distribution would introduce spurious variation into the residuals upon resampling for the bootstrap. The linear model for the heteroskedasticity is based on a Breusch-Pagan test for heteroskedasticity (Breusch-Pagan 1979), except it uses the absolute deviation. The normalization is identical to the normalization performed in a feasible weighted least squares heteroskedasticity correction (Cameron and Trivedi 2005). The heteroskedasticity stabilizing regression appears to have stabilized the variation as indicated by the more homogeneous variance (fig. B2). The heavy tails or extreme tail events of the normalized residual distribution is quite likely a feature of the true mortality error distribution which should be retained during resampling.

An implied assumption in this approach of the estimation variability for P_0 and α is that all variability comes from random error at the larval stage, $\varepsilon_{c,s}$ (equation 1).

Other potential sources of variation in P_0 and α were explored. The calculation of P_0 and the iterative method for α are simple definitional relationships and any error in the methods for the point estimates calculated after mortality estimation is negligible. The standing stock of eggs (m) and incubation time (t^1) are also used in HEP estimation and can potentially have a stochastic component. Reduced form attempts to model this stochasticity, that attempted to exploit the spatial variation over station within a year, were explored. A residual bootstrap method was again used with residual taken as deviation from a reduced form spatial model such as a spatial moving average process, spatial autoregressive process or a spatial distributed lag process. The results were that some additional variation was introduced but did not widen the confidence intervals for the parameters of interest significantly. The ad-hoc nature of this approach coupled within its marginal contribution led us to abandon this approach. Furthermore, aggregation over samples, cruises, and stations is likely to smooth the stochasitic components of m and t^1. Thus, we assume that the calculated values of m and t^1 are accurate annual statistics for the region in the sense that randomness in sampling or other sources is minimized by the aggregation. Alternatively, our bootstrapped distributions can be interpreted as conditional on the observed m and t^1.

Calculations of higher order moments (such as the variance) of the data can be particularly sensitive to extreme tail events. Thus, confidence intervals for parameter estimates can have poor coverage when constructed using standard errors based on a distribution prone to extreme tail events. The large standard error estimates for α_s and P_0 based on the delta method were likely the result of the heavy-tailed distributions. Furthermore, extreme events can also result in uncentered distributions. We obtain accurate coverage for parameter confidence intervals by reporting bootstrapped confidence intervals in place of the regression standard errors for the NLS estimation of MC^0 (equation 1).

APPENDIX B LITERATURE CITED

Breusch, T. and A. Pagan. 1979. A Simple Test for Heteroscedasticity and Random Coefficient Variation. Econometrica. 47:1287–1294.

Cameron, A. C. and P. K. Trivedi. 2005. Microeconometrics: methods and applications. Cambridge University Press.

Lo, N. C. H. 1985a. Egg production of the central stock of northern anchovy, *Engraulis mordax*, 1951–1982. Fishery Bulletin, 83:137–150.

MacKinnon, J. G. 2006. Bootstrapping methods in econometrics. The Economic Record. 82:S2–S18.